

## Spontaneous Article

<sup>10</sup>Be exposure age dating of Late Quaternary relative sea level changes and deglaciation of W Jura and NE Islay, Scottish Inner HebridesAlastair G. DAWSON<sup>1\*</sup> , Paul BISHOP<sup>2†</sup>, James HANSOM<sup>2</sup> and Derek FABEL<sup>3</sup><sup>1</sup> Geography and Environmental Science, Tower Building, University of Dundee, Dundee DD1 4HN, Scotland, UK.<sup>2</sup> School of Geographical and Earth Sciences, University of Glasgow, University Avenue, Glasgow G12 8QQ, Scotland, UK.<sup>3</sup> Scottish Universities Environmental Research Centre, East Kilbride, South Lanarkshire G75 0QF, Scotland, UK.\*Corresponding author. Email: [agdawson@dundee.ac.uk](mailto:agdawson@dundee.ac.uk)

**ABSTRACT:** New <sup>10</sup>Be exposure age dating and geomorphological mapping of emerged shoreline features in W Jura and NE Islay throw new light on the regional pattern of ice sheet deglaciation and late-glacial relative sea level change. We conclude that the oldest and highest emerged shorelines in this area were produced ~15.7–16.3 ka, shortly after ice sheet deglaciation ~16.5 ka. It is envisaged that the first incursion of marine waters into coastal areas took place close to a former ice sheet margin that oscillated in position across this part of the Scottish Inner Hebrides. The first evidence of late-glacial marine sedimentation following deglaciation consists of emerged marine terrace fragments and unvegetated gravel beach ridges, the former represented by a prominent glacio-isostatically tilted shoreline that declines in altitude NE to SW, from ~40 m above ordnance datum (OD) in NW Jura to ~19 m OD in central Islay. In W Jura, north of Loch Tarbert, spectacular staircases of up to 55 unvegetated gravel beach ridges were formed shortly after regional deglaciation, possibly within 1 ka. A preliminary estimate of the average rate of relative sea level lowering across W Jura between deglaciation and the Younger Dryas is in the order of ~7 mmyr<sup>-1</sup>. Geomorphological evidence from Shian Bay, W Jura, indicates a truncation of the late-glacial beach ridge staircases by a large 480-m-long beach ridge (the Colonsay Ridge) at ~14.9 ka, when former relative sea level was at ~18 m OD. This ridge may represent the product of either a stillstand in the progressive lowering of relative sea level during the late-glacial or a reversal. This raises the intriguing possibility of an association between ridge formation and the timing of the well-established global meltwater pulse 1A between ~14.65 and ~14.8 ka.



**KEY WORDS** <sup>10</sup>Be exposure dating, emerged beach ridges, emerged shorelines, glacio-isostatic rebound, global meltwater pulse 1A, ice sheet deglaciation, marine terraces, shore platforms.

The emerged beaches of W Jura and NE Islay in the Scottish Inner Hebrides are some of the finest examples of emerged shorelines in northern Europe, first described by Peach *et al.* (1911) and Wright (1928), as well as in several classic textbooks (e.g., Johnson 1922; Holmes 1965). The subject of numerous research papers (e.g., McCann 1961, 1964; Syngé & Stephens 1966; Dawson 1979, 1980, 1982; Dawson *et al.* 1997), the emerged shore features include shore platforms, cliffs, sea caves and marine terraces, together with spectacular staircases of vegetated and unvegetated gravel beach ridges (Figs 1, 2). As an assemblage, the coastal landforms provide a record of former relative sea level change, most of which has taken place since the melting of the last (Late Devensian) ice sheet.

In general, the study of emerged shoreline features in areas of glacio-isostatic rebound provides valuable information for two areas of Quaternary research. Firstly, detailed geomorphological mapping together with the measurement of the altitudes of emerged shoreline features and their dating can enable the

reconstruction of former patterns of the late-glacial relative sea level (RSL) change that accompanied the melting of the last ice sheet. A RSL curve exists for the Holocene on Islay (Dawson *et al.* 1998), but a lack of dateable material has hitherto prevented a relative sea level chronology for the Late Glacial (Dawson 1979, 1982; Dawson *et al.* 1997). Secondly, Late Quaternary sea level data are frequently used to reconstruct patterns of ice sheet deglaciation, the generation of such data being derived from carbon-14 (<sup>14</sup>C) dating and terrestrial cosmogenic nuclide dating (*cf.* Ballantyne & Small 2019). The present study reports cosmogenic <sup>10</sup>Be surface exposure ages of emerged beach ridges and associated deposits in W Jura and NE Islay, and informs our understanding of patterns of RSL change and glacio-isostatic adjustment following ice sheet deglaciation. All altitudes referred to herein are expressed in metres above ordnance datum (OD) Newlyn.

## 1. RSL change history

The age and origin of the emerged beach ridges examined here depend on accepted interpretations of their stratigraphic

<sup>†</sup>Deceased.

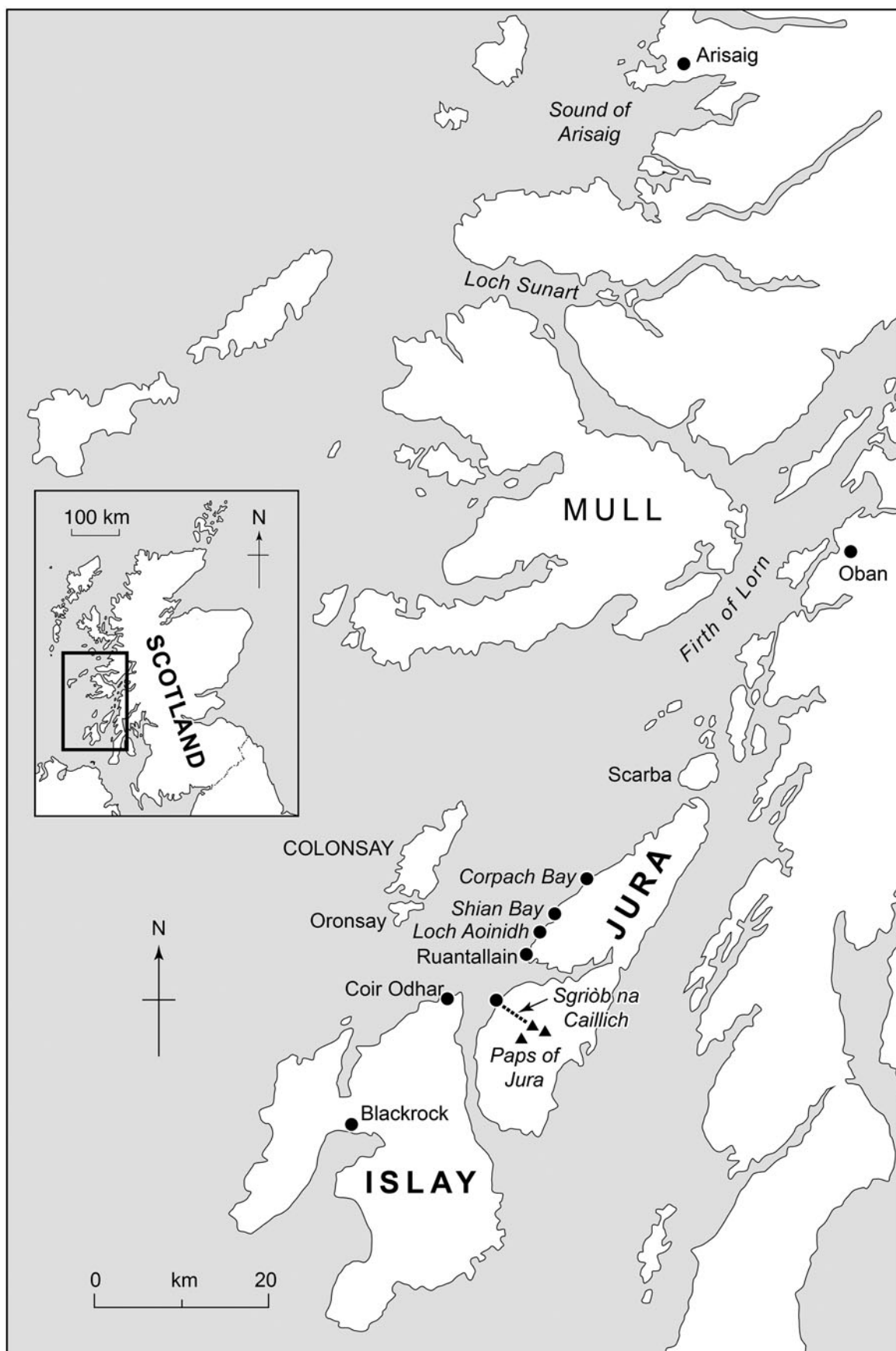


**Figure 1** Principal locations mentioned in text.

relationships with adjacent emerged shore platforms and glacio-genic sediments (Dawson *et al.* 1997). Broadly, there are two generations of emerged beach ridge sequences in Islay and Jura. The higher set rests upon a high-level emerged shore platform that is

continuously developed along the coastline of W Jura and N Islay. The platform is locally up to 600 m wide and backed by cliffs up to 90 m high, with a cliff–platform junction that varies along the coast between ~32 and ~34 m OD (Fig. 3). In W



**Figure 2** Oblique aerial photograph of late-glacial and Holocene-emerged gravel spreads in Loch Aoinidh area, western Jura. Note the termination seaward of the (higher) late-glacial beach ridge staircases at the top of the cliff of the Main Rock Platform. Photo courtesy of E Smith (photo reference ezs DSC\_9787).

Jura, this higher set of beach ridges is locally underlain by glacial till that, in turn, rests upon the emerged rock platform surface and demonstrates that the formation of this shore platform

and the deposition of the beach ridges are separated by at least one period of general glaciation. It is also generally recognised that this high set of beach ridges is likely to have been deposited immediately following the deglaciation of the last (Late Devensian) ice sheet in Jura and Islay (McCann 1961; Syngé & Stephens 1966; Dawson 1982; Dawson *et al.* 1997) at *ca.*16.5 ka (Small *et al.* 2017).

The second set of emerged beach ridges occur at lower altitudes immediately inland from the present coastline (Figs 2–4). All of these ridges rest upon a lower emerged shore platform that can be traced as a virtually continuous feature along the coastline of W Jura and N Islay. This platform is typically 100–150 m wide and terminates inland at a cliff whose top forms the seaward edge of the higher rock platform described above (Fig. 3). The higher and lower shore platforms are both crudely planated rock surfaces composed mostly of inclined ridges of Proterozoic quartzite interrupted locally by Tertiary dolerite dykes. The emerged beach ridges that rest upon the lower platform surface are generally fragmentary and interpreted as Holocene in age since they rest on an underlying platform (the Main Rock Platform), which is late-glacial in age, having been formed by cold-climate shore erosion processes during the Younger Dryas (*ca.*12.9–11.7 ka) (Dawson 1979, 1980; Stone *et al.* 1996; Lowe *et al.* 2019) (Fig. 3). This platform and cliff are part of a more widespread

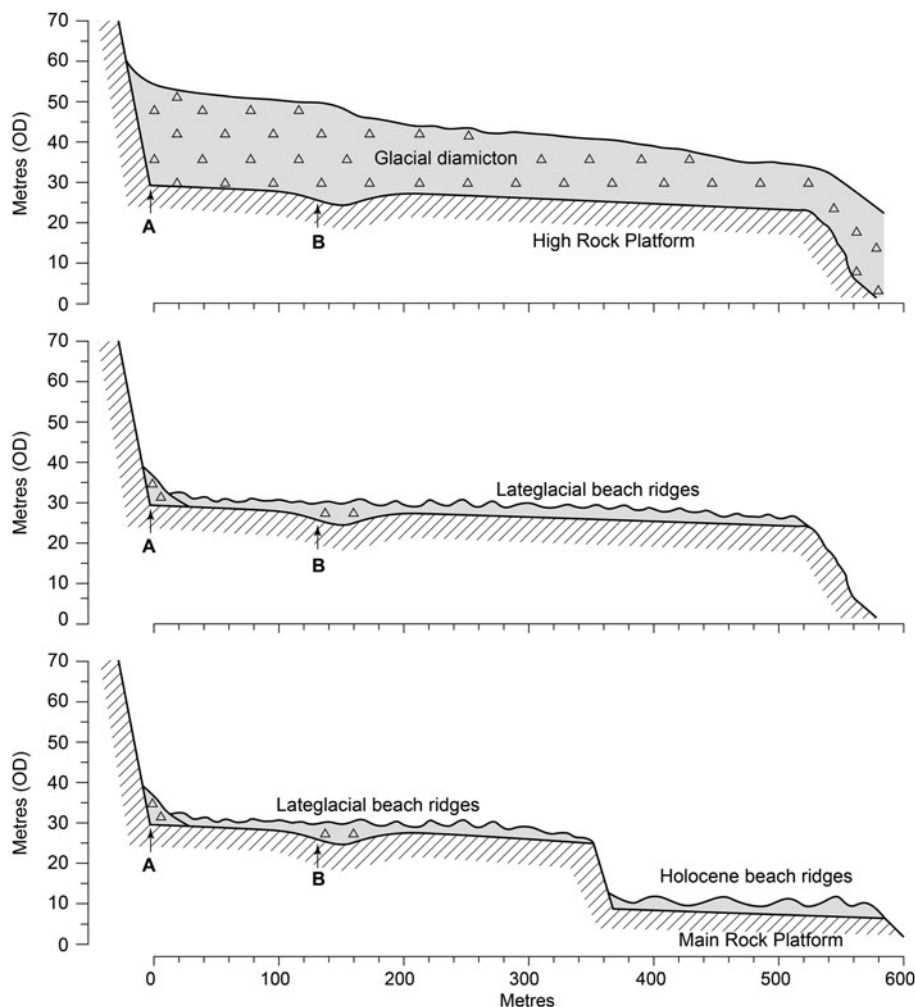


**Figure 3** Three-stage schematic diagram of coastline evolution, W Jura. Top and middle: note that the deposition of the late-glacial beach ridges took place as a result of the erosion and winnowing of glacial sediments by the late-glacial sea across a much more extensive High Rock Platform. Bottom: a lower emerged shore platform was produced rapidly during the Younger Dryas as a result of cold-climate coastal processes that led to the seaward truncation of the (higher) late-glacial beach ridge staircases. Glacial till at locations A and B demonstrate that the late-glacial beach gravels and underlying High Rock Platform are separated by a period of ice sheet glaciation. Not to scale.



**Figure 4** Oblique aerial photograph of late-glacial and Holocene-emerged gravel spreads, Shian Bay, western Jura. Photo courtesy of E Smith (photo reference ezs DSC 9780).

emerged shoreline that is well-developed across extensive areas of western Scotland. The feature exhibits glacio-isostatic tilting across Jura and Islay with a maximum altitude of  $\sim 6$  m OD in N Jura, 3 m OD in W Jura and passes below present sea level in NE Islay (Dawson 1980).

In W Jura, the higher set of emerged beaches is represented by spectacular staircases of both unvegetated and vegetated gravel ridges with intervening swales. For example, at Loch Aoinidh, a  $\sim 650$ -m-wide sequence of 55 unvegetated curvilinear ridges and swales descends seaward as far as the top of the Main Rock Platform cliff line at  $\sim 20$  m OD (Fig. 2). In most areas, the highest beach ridges occur adjacent to narrow emerged marine terrace fragments that define the marine limit, the highest RSL reached by the late-glacial sea following regional deglaciation (Fig. 5). These terrace fragments can be traced along the coast as almost continuous features and represent a single emerged shoreline with marked regional variations in altitude reflecting differential glacio-isostatic adjustment. This tilted shoreline, representing the marine limit, now lies at elevations of  $\sim 40$  m OD at Corpach Bay in NW Jura,  $\sim 35$  m OD between Ruantallain and Shian Bay,  $\sim 26$ – $27$  m OD in NE Islay and at  $\sim 19$  m OD at Blackrock in central Islay (Fig. 1). During regional deglaciation, the formation of these emerged marine terraces was followed by the progressive deposition of staircases of beach ridges during a period of RSL lowering when glacio-isostatic rebound outpaced the glacio-eustatic rise in sea level caused by the melting of ice sheets worldwide (Lambeck *et al.* 2014). In NE Islay, an arcuate moraine located adjacent to a raised marine terrace at Coir Odhar has been associated with radically different interpretations in respect of its age and origin (Fig. 1). One view was that the moraine was produced during a readvance of ice during the Loch Lomond Stadial (Younger Dryas) (McCann 1964), while another was that the moraine represented one of a series of drift ridges produced during ice sheet deglaciation and that the marine terrace was formed shortly following deglaciation (Synge & Stephens 1966; Dawson 1979).

Following the end of the Younger Dryas, the rate of glacio-eustatic sea level rise caused by the worldwide melting of ice sheets began to exceed the local rate of glacio-isostatic rebound. As a result, a rise in RSL took place throughout the early Holocene, culminating in Islay at *ca.* 5 ka (Dawson *et al.* 1998). Thereafter, the remainder of the Holocene in Jura and Islay was characterised by residual glacio-isostatic rebound, together with the deposition of the lower sets of Holocene-emerged beach ridges.

## 2. Methodology

### 2.1. Geomorphological mapping

Geomorphological mapping presented here was validated with earlier 1:10,000 field mapping (Dawson 1979), and later updated for Islay (Dawson 1982) using ground survey and aerial photography. The altitudes of all emerged features were initially surveyed to UK Liverpool datum, with all traverses completed with closing errors of no greater than 10 cm. A separate survey between Liverpool and Newlyn Ordnance Survey benchmarks ensured that all altitudes reported here refer to Newlyn datum (OD). The altitudes and GPS locations of those emerged ridge whose gravels were sampled and used to calculate  $^{10}\text{Be}$  exposure ages for dating purposes were also cross-checked against aerial photography and the mapped positions of emerged shoreline features.

The surveyed heights of all emerged marine terrace fragments were plotted on shoreline height-distance diagrams constructed normal to the shoreline uplift isobases, to allow individual shorelines and beach ridge features to be distinguished from each other. The altitudes of all vegetated and unvegetated beach ridges were also surveyed to OD, with the crest altitudes of prominent individual ridges being determined at several points along their length. Where individual ridges formed part of a staircase of ridges, the altitudes of individual swales separating pairs of ridges were determined at multiple points along their lengths to allow ridge and swale profiles to be constructed.

At all sites, the altitude, latitude and longitude were recorded using a handheld Garmin 60Csx GPS. At several sites, two samples of emerged gravels were collected – a single large clast (15 cm *b*-axis) and 4–5 smaller clasts (5 cm *b*-axis) – to test whether grain size influences the cosmogenic nuclide concentration. All samples were selected randomly. On the unvegetated emerged beach ridges, only ridges that were too coarse-grained and well-drained to have ever supported the development of covering peat were sampled (Table 1). Where sampling involved moraine or glacialfluvial terraces grading to well-defined emerged marine features, the depth of peat overlying the uppermost gravels was measured to allow a shielding factor to be included into the exposure age calculation. Topographic shielding was measured in the field using a compass and clinometer (Table 1). Since clasts will have some amount of nuclide inheritance prior to final deposition dependent on how long they reside in swash zone before final deposition, we estimated the cosmogenic nuclide concentration accumulated prior to deposition by sampling similar size and shape clasts from deep within three abandoned sea caves (two at  $\sim 5$  m to the rear of the present beach, the other at  $\sim 13$  m) (Tables 1, 2). After a sample is deposited within a cave, cosmogenic nuclide production is reduced to  $<0.4\%$  due to shielding by 15–20 m of overlying rock. Thus, the measured cosmogenic nuclide concentrations in cave clasts provides a minimum constraint on inheritance due to residence time in the swash zone. The clast may have been active in the cave for a period of time while accumulating negligible amounts of  $^{10}\text{Be}$ , and so its  $^{10}\text{Be}$  inventory could underestimate the true amount of inheritance of clasts elsewhere in the system.

The quartzite gravel samples were crushed and sieved, and the 250–500  $\mu\text{m}$  fraction was cleaned with aqua regia. Approximately 80 g of the samples was etched multiple times in 2% hydrofluoric acid to remove the minor amounts of non-quartz contaminants and to remove any meteoric  $^{10}\text{Be}$  that may have adhered to grain surfaces (Kohl & Nishiizumi 1992). Quartz purity was assayed and the clean quartz fractions were split between two laboratories to prepare targets for accelerator mass spectrometry. The Jura samples were processed in the Natural Environment Research Council (NERC) Cosmogenic Isotope Analysis Facility, and the Islay samples in the Scottish

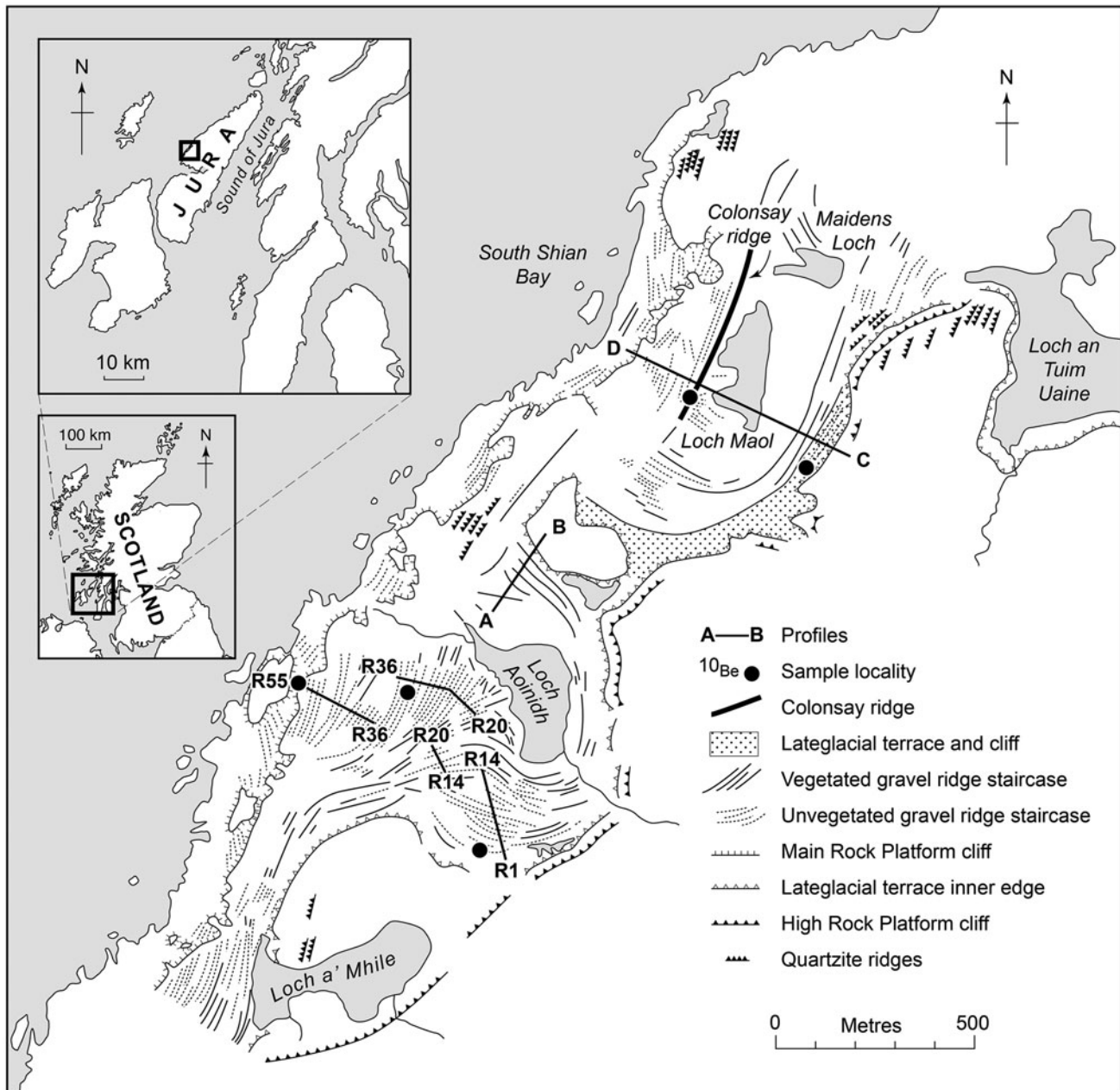


**Figure 5** Geomorphological map of raised shoreline features, Loch Aoinidh, W Jura, showing locations of <sup>10</sup>Be samples used to reconstruct pattern of late-glacial RSL changes (see Fig. 11). In this area, a High Rock Platform is locally mantled by staircases of unvegetated emerged beach ridges that extend up to ~36 m OD. The ridges terminate seaward at an emerged cliff and shore platform of Younger Dryas age (the Main Rock Platform). Note also that this emerged platform is mantled by Holocene beach gravels (see also Fig. 2). Note also the well-defined 480-m-long linear beach ridge, the Colonsay Ridge, whose seaward base lies at ~18 m OD (see Fig. 4). Topographic profiles and location of the beach ridge staircases at Loch Aoinidh together with profiles A–B and C–D are shown in Figures 7 and 8.

Universities Environmental Research Centre (SUERC) Cosmogenic Nuclide Laboratory. Three samples (I04, I06 and I07) were shared to check interlaboratory compatibility. The samples were spiked with between 166 and 285 µg of <sup>9</sup>Be carrier before being dissolved in 48% w/w hydrofluoric acid (HF). Matrix contaminants (iron, calcium, titanium) were removed using ion chromatography. Beryllium hydroxide was precipitated, calcined at 900 °C and the final beryllium oxide (BeO) sample mixed with a niobium binder (BeO: Nb = 1:6) before being pressed into target cathodes for Accelerator mass spectrometry (AMS) measurement.

AMS targets were measured at the SUERC AMS Laboratory (Freeman *et al.* 2007; Xu *et al.* 2010). <sup>10</sup>Be/<sup>9</sup>Be ratios (Table 2) were normalised to the NIST4325 standard reference material (<sup>10</sup>Be/<sup>9</sup>Be ratio of  $2.79 \times 10^{-11}$ ; Nishiizumi *et al.* 2007). All isotopic ratios were corrected using full chemistry procedural blanks. Background corrections ranged between 3% and 60%

of the measured AMS <sup>10</sup>Be/<sup>9</sup>Be ratio (Table 2). Final analytical errors in <sup>10</sup>Be concentration (<sup>10</sup>Be atom/g-quartz) were derived from the quadrature addition of the uncertainty in the AMS ratio, and a 2% uncertainty in Be-spike assay resulting in a combined analytical error ranging from 4% to 5.8% (Table 2).

<sup>10</sup>Be surface exposure ages were calculated using version 3 of the online exposure age calculator described by Balco *et al.* (2008, 2013) and subsequently updated (<http://hess.ess.washington.edu/>; wrapper: 3.0.2; get\_age: 3.0.2; muons: 1A,  $\alpha = 1$ ; validate: validate\_v3\_input.m – 3.0; consts: 3.0.4). The ages presented in Table 1 are based on the scaling method (Lifton *et al.* 2014), and two calibration data sets – the CRONUS Primary Be-10 calibration data set (Borchers *et al.* 2016), and a local <sup>10</sup>Be calibration dataset (LLPR) derived from <sup>10</sup>Be concentrations in samples from boulders on the Younger Dryas terminal moraine at the southern end of Loch Lomond, ~95 km ENE of Jura

**Table 1** Grid reference location data, altitude values and shielding parameter values for  $^{10}\text{Be}$  samples used in this study.

Sample ID	Description	Latitude (degrees N)	Longitude (degrees E)	Elevation (m OD)	Sample thickness (cm) (shielding factor) <sup>1</sup>	Topographic shielding factor <sup>2</sup>	Peat/sand depth (cm) (shielding factor) <sup>3</sup>
Cave1	Cave sample on Jura	55.99744	-5.99035	13	5 (0.959)	1	1
Cave2A	Cave sample on Jura	55.99466	-5.99234	5	6 (0.951)	1	1
I08cave	Cave sample on Islay	55.934773	-6.13851	5	8 (0.9354)	1	1
Scriob	Scriob na Caillich medial moraine (Small <i>et al.</i> 2017, recalculated)	55.91763	-6.05086	106	1 (0.9916)	0.9995	1
LOCHA01A	Loch Aonidh, high level, large cobble	55.99593	-5.98134	36	15 (0.8835)	0.999	1
LOCHA01B	Loch Aonidh, high level, five small cobbles	55.99593	-5.98134	36	5 (0.959)	0.999	1
LOCHA02A	Loch Aonidh, mid-level, large cobble	55.9995	-5.98452	34	15 (0.8835)	0.9998	1
LOCHA02B	Loch Aonidh, mid-level, five small cobbles	55.9995	-5.98452	34	5 (0.959)	0.9998	1
LOCHA03A	Loch Aonidh, prominent ridge on top of MRP, large cobble	55.99935	-5.9884	28	15 (0.8835)	0.9983	1
LOCHA03B	Loch Aonidh, prominent ridge on top of MRP, small cobbles	55.99935	-5.9884	28	5 (0.959)	0.9983	1
LOCHA04A	Loch Aonidh, Holocene ridge, large cobble	55.99986	-5.98851	11	15 (0.8835)	0.9988	1
LOCHA04B	Loch Aonidh, Holocene ridge, small cobbles	55.99986	-5.98851	11	5 (0.959)	0.9988	1
HS01A	Shian Bay, high shoreline, large cobble, fractured	56.0047	-5.96922	36	15 (0.8835)	0.9983	1
HS01B	Shian Bay, high shoreline, five small cobbles	56.0047	-5.96922	36	5 (0.959)	0.9983	1
ShianTrig	Ice-moulded bedrock	56.00764	-5.9641	71	1 (0.9916)	1	1
LS02A	Shian Bay, low shoreline, large cobble	56.00708	-5.97535	13	15 (0.8835)	0.9997	1
LS02B	Shian Bay, low shoreline, four small cobbles	56.00708	-5.97535	13	5 (0.959)	0.9997	1
LS01A	Shian Bay, Holocene shoreline, large cobble	56.00789	-5.97582	8	15 (0.8835)	0.9994	1
LS01B	Shian Bay, Holocene shoreline, four small cobbles	56.00789	-5.97582	8	5 (0.959)	0.9994	1
MS01A	Colonsay Ridge, large cobble	56.00613	-5.97364	18	15 (0.8835)	0.9997	1
MS01B	Colonsay Ridge, four small cobbles	56.00613	-5.97364	18	5 (0.959)	0.9997	1
SB1	Beach ridge truncating Scriob na Caillich medial moraine, large cobble	55.92177	-6.0584	30	15 (0.8835)	0.9998	1
SB2	Beach ridge truncating Scriob na Caillich medial moraine, small cobbles	55.92177	-6.0584	30	5 (0.959)	0.9998	1
I03	Outwash gravel on glacial outwash terrace	55.92666	-6.16142	40	3 (0.9751)	0.9976	21 (0.993)
I04*	Outwash gravel over platform below 36.5 cm peat	55.92751	-6.1628	35	3 (0.9751)	0.9976	36.5 (0.9882)
I04ciaf*	Outwash gravel over platform below 36.5 cm peat	55.92751	-6.1628	35	3 (0.9751)	0.9976	36.5 (0.9882)
I04mean							
I07*	Holocene beach cobbles under 5 cm sand	55.9325	-6.14869	15	3 (0.9751)	0.9582	5 (0.9709)
I07ciaf*	Holocene beach cobbles under 5 cm sand	55.9325	-6.14869	15	3 (0.9751)	0.9582	5 (0.9709)
I07mean							

\*Samples split and processed in separate laboratories; NERC Cosmogenic Isotope Analysis Facility and SUERC Cosmogenic Nuclide Laboratory.

<sup>1</sup>Sample thickness (cm) and shielding factor (in brackets) calculated using a rock density of  $2.7 \text{ g cm}^{-3}$  and a cosmic-ray attenuation length of  $160 \text{ g cm}^{-2}$ .

<sup>2</sup>Calculated according to Dunne *et al.* (1999).

<sup>3</sup>Correction for shielding by sand (density  $1.8 \text{ g cm}^{-3}$ ) and peat (density  $0.7 \text{ g cm}^{-3}$ ), assuming peat thickness increased linearly during the last 2 ka of exposure.

(Fabel *et al.* 2012). The age of this moraine is independently constrained by radiocarbon dating (MacLeod *et al.* 2011). The advantage of using a local calibration data set is that it minimises production rate scaling by inferring production rates from sites that are close in paleomagnetic field characteristics, elevation and age to the unknown-age sites being dated. Using a local calibration data set is, therefore, less subject to production rate scaling uncertainties than extrapolating production rates inferred from a globally distributed set of calibration data to parts of location-age space that are not well represented by the calibration sites (Balco 2013). Therefore, the LLPR derived ages and full uncertainties are used here. We do not include atmospheric pressure anomalies and assume no significant erosion of the quartzite gravels during exposure ( $\epsilon = 0 \text{ mm a}^{-1}$ ), and no prior exposure except in the swash zone, as noted above. The samples on Islay were collected from under a relatively shallow (<37 cm) peat cover. Fulop *et al.* (2015) demonstrated that a 15–30-cm-thick peat developed on a

moraine ~95 km to the ENE of our sample sites started forming at a maximum of ~2000 years BP. Assuming the same bulk density of  $0.5\text{--}0.9 \text{ g cm}^{-3}$ , and linear growth for 2000 years, the maximum peat cover (36.5 cm) reduces cosmogenic nuclide production in the immediately underlying beach gravels by 6–10% during the last 2000 years of exposure. Although shielding by peat cover only influences the ages by 0.7–1.2%, it has been included for the peat covered samples.

### 3. $^{10}\text{Be}$ beach ridge surface exposure dating and chronology

#### 3.1. Dating constraints

Two cave samples collected at 5 m OD just above the active gravel beaches (Cave 2A and the I08 cave; Tables 1, 2) have similar  $^{10}\text{Be}$  concentrations, with an uncertainty weighted mean of  $6022 \pm$

**Table 2** Dissolved quartz mass values, <sup>9</sup>Be, <sup>10</sup>Be and exposure age data used in this study

Sample ID	Quartz mass dissolved (g)	<sup>9</sup> Be (μg)	<sup>10</sup> Be/ <sup>9</sup> Be (×10 <sup>-15</sup> ) <sup>1</sup>	Process blank <sup>10</sup> Be (×10 <sup>4</sup> atoms) <sup>2</sup>	<sup>10</sup> Be (×10 <sup>4</sup> atom g <sup>-1</sup> ) <sup>3</sup>	Exposure age using default calibration data set (ka) <sup>4</sup>	Exposure age using local calibration data set (ka) <sup>4</sup>	Inheritance-adjusted exposure age using local calibration data set (ka) <sup>5</sup>	Exposure age used in text (ka)
Cave1	27.056	295.5 ± 5.9	7.62 ± 1.08	10.5 ± 1.5	0.17 ± 0.1				
Cave2A	20.031	247.5 ± 4.9	10.11 ± 1.01	4.2 ± 1.3	0.62 ± 0.11				
I08cave	23.533	248.2 ± 5	11.59 ± 1.56	5.7 ± 1.2	0.57 ± 0.12				
Scriob	18.527	247.3 ± 4.9	92.2 ± 3.4	4.2 ± 1.3	8 ± 0.36				16.5 ± 0.9
LOCHA01A	30.67	253.4 ± 5.1	153.4 ± 8.2	9.4 ± 1.5	8.16 ± 0.49	19.8 ± 1.7	21.4 ± 1.4	20.9 ± 1.4	16.3 ± 0.9
LOCHA01B	29.5281	254.1 ± 5.1	125.9 ± 4.9	9.4 ± 1.5	6.92 ± 0.32	15.5 ± 1.2	16.8 ± 0.9	16.3 ± 0.9	
LOCHA02A	30.5688	253.3 ± 5.1	130 ± 4.9	9.4 ± 1.5	6.89 ± 0.31	16.8 ± 1.3	18.1 ± 0.9	17.6 ± 1.0	16.2 ± 0.9
LOCHA02B	29.6446	254.3 ± 5.1	125.1 ± 4.6	9.4 ± 1.5	6.85 ± 0.3	15.4 ± 1.1	16.6 ± 0.8	16.2 ± 0.9	
LOCHA03A	28.0392	285.1 ± 5.7	96.2 ± 3.1	9.5 ± 1.3	6.2 ± 0.25	15.2 ± 1.1	16.4 ± 0.8	15.9 ± 0.8	15.3 ± 0.8
LOCHA03B	28.3978	285 ± 5.7	101.3 ± 3.5	9.5 ± 1.3	6.46 ± 0.28	14.6 ± 1.1	15.7 ± 0.8	15.3 ± 0.8	
LOCHA04A	29.9372	251.5 ± 5	34.4 ± 2	6 ± 0.9	1.73 ± 0.12	4.3 ± 0.4	4.6 ± 0.3	3 ± 0.4	3.0 ± 0.4
LOCHA04B	28.0244	285.8 ± 5.7	23.3 ± 1.5	9.5 ± 1.3	1.25 ± 0.11	2.8 ± 0.3	3.0 ± 0.3	1.5 ± 0.3	1.5 ± 0.3
HS01A	29.7606	253.8 ± 5.1	130.9 ± 5.7	9.4 ± 1.5	7.14 ± 0.36	17.4 ± 1.4	18.7 ± 1	18.3 ± 1.1	15.7 ± 0.9
HS01B	29.972	252.4 ± 5	124.2 ± 5	9.4 ± 1.5	6.68 ± 0.32	15 ± 1.1	16.2 ± 0.9	15.7 ± 0.9	
ShianTrig	20.109	247.6 ± 5	86.68 ± 4	5.11 ± 1.72	6.88 ± 0.37	14.4 ± 1.2	15.6 ± 0.9	15.6 ± 0.9	15.6 ± 0.9
LS02A	29.7622	283.2 ± 5.7	34.3 ± 1.9	8.9 ± 1.1	1.88 ± 0.14	4.7 ± 0.4	5 ± 0.4	3.4 ± 0.4	3.4 ± 0.4
LS02B	30.0588	285.2 ± 5.7	46.5 ± 4	8.9 ± 1.1	2.65 ± 0.26	6.1 ± 0.7	6.6 ± 0.7	5.1 ± 0.7	5.1 ± 0.7
LS01A	32.4044	254 ± 5.1	18.6 ± 2.3	9.4 ± 1.5	0.68 ± 0.13	1.6 ± 0.3	1.8 ± 0.3	0.2 ± 0.4	0.2 ± 0.4
LS01B	30.0638	284.6 ± 5.7	34.5 ± 2	8.9 ± 1.1	1.88 ± 0.14	4.3 ± 0.4	4.7 ± 0.4	3.1 ± 0.4	3.1 ± 0.4
MS01A	30.1177	284.1 ± 5.7	107.8 ± 4.3	8.9 ± 1.1	6.5 ± 0.3	16.1 ± 1.2	17.3 ± 0.9	16.9 ± 0.9	14.9 ± 0.8
MS01B	31.5781	281.3 ± 5.6	109.1 ± 4.1	8.9 ± 1.1	6.21 ± 0.28	14.2 ± 1.1	15.3 ± 0.8	14.9 ± 0.8	
SB1	30.3765	285.2 ± 5.7	134 ± 4.5	8.9 ± 1.1	8.12 ± 0.33	19.6 ± 1.4	21.2 ± 1	20.9 ± 1	14.5 ± 0.8
SB2	29.9738	282.8 ± 5.7	102.1 ± 3.8	8.9 ± 1.1	6.14 ± 0.27	13.7 ± 1	14.8 ± 0.7	14.5 ± 0.8	
I03	23.244	256.7 ± 5.1	76.5 ± 2.7	8.1 ± 1.5	5.3 ± 0.24	11.8 ± 0.9	12.7 ± 0.6	12.7 ± 0.6	12.7 ± 0.6
I04*	26.501	252.4 ± 5	75.3 ± 3.6	4.2 ± 1.3	4.63 ± 0.26	10.4 ± 0.8	11.2 ± 0.7	11.2 ± 0.7	10.8 ± 0.4
I04ciaf*	17.7507	177.3 ± 3.5	72.2 ± 2.2	8.2 ± 0.8	4.36 ± 0.18	9.8 ± 0.7	10.5 ± 0.5	10.5 ± 0.5	
I04mean					4.45 ± 0.15	10.0 ± 0.7	10.8 ± 0.4	10.8 ± 0.4	
I07*	28.801	256.3 ± 5.1	35.14 ± 2.87	8.1 ± 1.5	1.81 ± 0.18	4.4 ± 0.5	4.7 ± 0.5	4.3 ± 0.5	4.3 ± 0.5
I07ciaf*	13.4761	166.1 ± 3.3	27.87 ± 1.48	8.2 ± 0.8	1.69 ± 0.14	4.1 ± 0.4	4.4 ± 0.4	3.9 ± 0.4	3.9 ± 0.4
I07mean					1.73 ± 0.11	4.2 ± 0.4	4.5 ± 0.3	4.1 ± 0.3	4.1 ± 0.3

<sup>1</sup>Isotope ratios were normalised to NIST SRM 4325 using <sup>10</sup>Be/<sup>9</sup>Be = 2.79 × 10<sup>-11</sup>.

<sup>2</sup>Atoms of <sup>10</sup>Be in the <sup>9</sup>Be carrier.

<sup>3</sup>Blank corrected <sup>10</sup>Be concentration. Propagated uncertainties include uncertainties in the process blank, carrier mass and counting statistics.

<sup>4</sup>Calculated with the CRONUS-Earth online calculator (Balco *et al.* 2008) version 3 (wrapper: 3.0.2; get\_age: 3.0.2; muons: 1A, α = 1; validate: validate\_v3\_input.m - 3.0; consts: 3.0.4; <http://hess.ess.washington.edu/>), using the LSDn scaling method. Uncertainties include analytical and production rate uncertainties reported at 1 sigma confidence level.

<sup>5</sup>Inheritance-adjusted exposure ages calculated after subtracting the mean <sup>10</sup>Be concentration of the lower cave samples from the <sup>10</sup>Be concentration in the beach cobble samples below 14 m above sea level and the mean <sup>10</sup>Be concentration of the upper cave sample from the <sup>10</sup>Be concentration in the beach cobble samples at and above 14 m above sea level.

810 atom g<sup>-1</sup>. The third cave sample (Cave 1), collected from a higher elevation cave deposit (13 m OD), has a much lower <sup>10</sup>Be concentration (1673 ± 962 atom g<sup>-1</sup>). The <sup>10</sup>Be concentration in the higher elevation cave sample implies a short residence time in the swash zone prior to deposition (about 400 years or so). This could be due to more rapid RSL lowering at the time of deposition, or deposition in a brief period of cave reactivation during a period of Holocene RSL rise observed elsewhere along the Scottish west coast (Shennan *et al.* 2006). Since beach ridges deposited above this sample location are likely to have been deposited during a period of more rapidly falling RSL, we subtract the <sup>10</sup>Be concentration of the higher elevation cave sample from all beach ridge samples at and above 14 m OD, and acknowledge that the 400 years value may well overestimate the residence time over the earlier period of RSL fall. For samples below 14 m OD, we subtract the mean of the <sup>10</sup>Be concentration in the lower two cave samples. The inheritance adjusted exposure ages are used in the text (Table 2).

The timing of deglaciation across SW Jura is well constrained by five <sup>10</sup>Be dates on boulders that comprise part of the Sgriob na Caillich medial moraine (Fig. 6; Table 2) (Ballantyne *et al.* 2014; Small *et al.* 2017; Ballantyne & Dawson 2019). Collectively, the

exposure ages for two medial moraine boulder samples collected by Ballantyne *et al.* (2014) and three boulder samples collected during this study (S1, S2, S3) published in Small *et al.* (2017) yield an arithmetic mean exposure age of 16.5 ± 0.8 ka. Here, we use the ~16.5 ka age as the reference age for deglaciation and assume that all <sup>10</sup>Be exposure ages for the Jura and Islay emerged beach gravels are younger. <sup>10</sup>Be exposure ages of five single largest clasts (>15 cm *b*-axis) on five of the highest beach ridges uniformly yield ages older than ~16.5 ka, even after the inheritance derived from the cave samples is subtracted. Accordingly, these five sample ages are discounted from this study (Table 2).

The ages from amalgamated smaller clasts sampled from individual emerged ridges are likely to reflect more surface abrasion than larger clasts due to more frequent movement in the source swash zone. They are thus less likely to exhibit inheritance and so may provide a more accurate constraint on emerged beach age. In addition, there may also be greater local post-depositional shielding of smaller clasts by surrounding larger clasts. Both effects – abrasion and, to a lesser extent, shielding – serve to lower the measured nuclide concentration, reduce the effect of inheritance and provide some degree of confidence in their

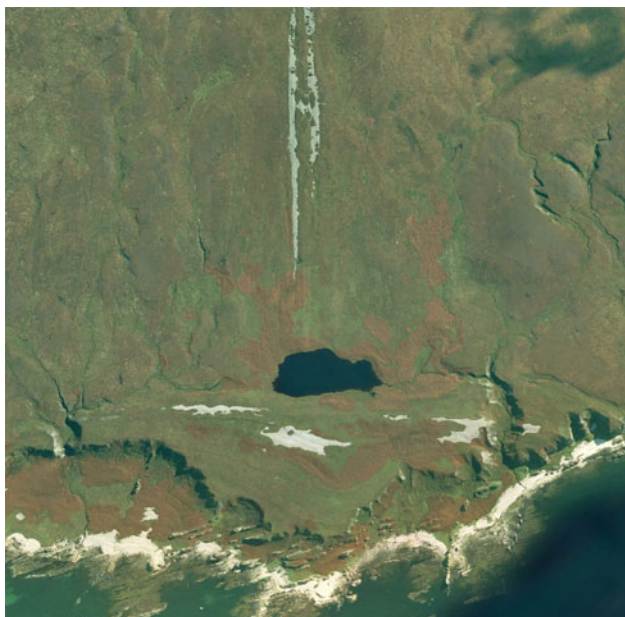


**Figure 6** Vertical Google Earth image (18.02.22) of Sgriob na Caillich medial moraine, SW Jura. At the seaward end of the hillslope, Loch na Sgrioba separates the moraine from an unvegetated emerged gravel ridge that cuts across the moraine at right angles (see also Fig. 10).

ages. However, the three samples from Holocene beach ridges do not show the same trend (Table 2) and it may be that the older ages in all samples where the comparison can be made include material that has been remobilised from older beach ridges.

### 3.2. Chronology

**3.2.1. Loch Aoinidh.** The age of the highest level reached by the late-glacial sea across W Jura as deglaciation commenced was estimated using the  $^{10}\text{Be}$  content of quartzite cobbles from the unvegetated gravel ridges landward of Loch Aoinidh and at the rear of the Shian Bay embayment (Figs 5, 7; Table 2). At Loch Aoinidh, age determinations were made of an emerged beach ridge crest R1 (~36 m OD) adjacent to a high-level late-glacial marine terrace fragment at 35.1 m. The  $^{10}\text{Be}$  age for five cobbles sampled from the ridge crest is  $16.3 \pm 0.9$  ka and is

interpreted here as the likely date of a RSL at *ca.*35.1 m OD (Figs 5, 7; Table 2: samples LOCHA01).

Two additional dates were obtained for quartzite cobbles on three ridge crests sampled from the 55-ridge sequence at Loch Aoinidh (Fig. 7; Table 2). The crest of the 25th ridge in the staircase lies at ~28.2 m OD, while the swale immediately seaward is at ~28.0 m OD. The altitude of this swale located adjacent to and seaward of this ridge is considered a relatively accurate indicator of former high-water mark at the time of ridge formation. The five cobbles sampled from this ridge provided an age of  $16.2 \pm 0.9$  ka (Table 2: samples LOCHA02). A separate date of  $15.3 \pm 0.8$  ka was obtained for five cobbles sampled from ridge 51 at the seaward end of the sequence (Fig. 6; Table 2: samples LOCHA03). This ridge has a crest altitude of ~21.3 m, with the altitude of the swale immediately seaward of it slightly lower at ~20.8 m OD. Our interpretation is that ridge 51 was deposited at ~15.3 ka when RSL had fallen to ~21 m OD.

Lying at 11 m OD at Loch Aoinidh, additional dates were obtained from quartzite cobbles on the Holocene-emerged beaches located below the Main Rock Platform cliff (Tables 1, 2: samples LOCHA04). These provided ages of  $3.0 \pm 0.4$  ka and  $1.5 \pm 0.3$  ka, the age discrepancy indicating that such beaches may still be within reach of modern storm waves that introduce modern clasts into the older beach ridges.

**3.2.2. Shian Bay.** A  $^{10}\text{Be}$  surface exposure age was also obtained for five cobbles sampled from beach ridge R1, the highest late-glacial unvegetated gravel ridge (~36.2 m OD) located at the rear of the Shian Bay embayment (Figs 4, 8; Table 2: samples HS01). This ridge is also located adjacent to a well-defined marine terrace fragment, the inner edge of which is at 36.3 m, and provided an age of  $15.7 \pm 0.9$  ka. The  $^{10}\text{Be}$  exposure age on a sample from an area of ice-moulded bedrock immediately landward of Shian Bay (NR 52988650) gave an age of  $15.6 \pm 0.9$  ka (Table 2: sample Shian Trig).

Located at 13 m and 8 m OD at Shian Bay, additional dates were obtained from quartzite cobbles on Holocene-emerged beaches located below the Main Rock Platform cliff (Tables 1, 2: samples LS02). At 13 m OD, these provided ages of  $3.4 \pm 0.4$  ka and  $5.1 \pm 0.7$  ka, whilst the dates at 8 m OD were  $3.1 \pm 0.4$  ka and  $0.2 \pm 0.4$  ka, again the age discrepancy suggesting the presence of more recently introduced cobbles alongside original ones at altitudes within reach of modern storm waves (Table 2: samples LS01).

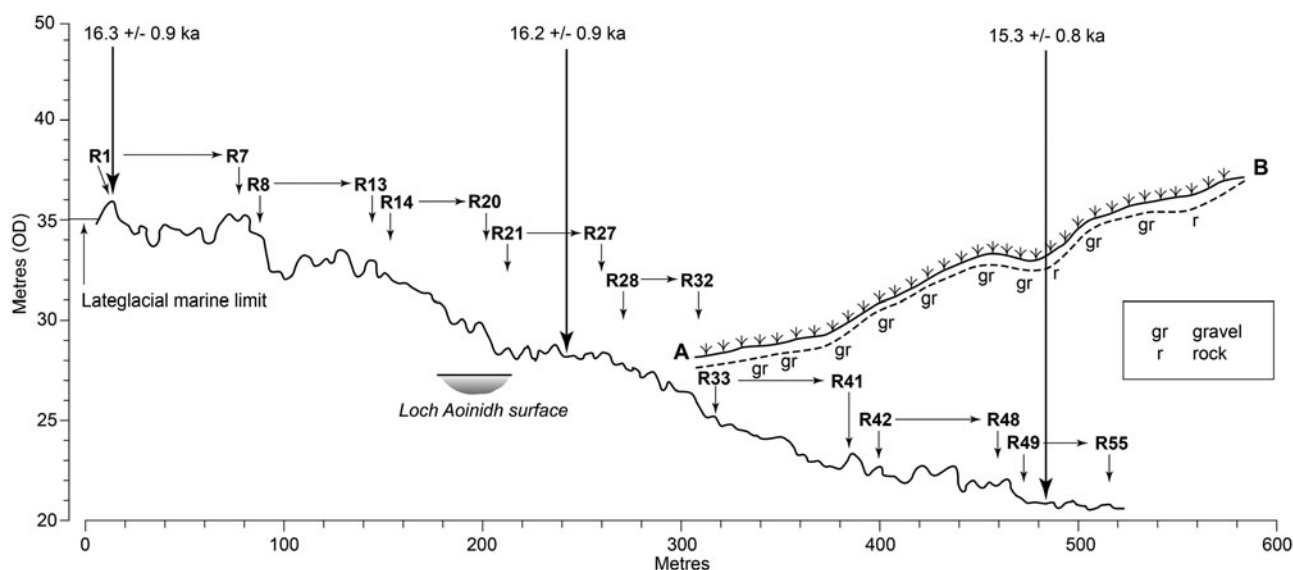


**Figure 7** Cross profile of the 55 beach ridge staircase sequence at Loch Aoinidh, W Jura. A shorter profile across a staircase of vegetated beach ridges, A–B is also shown (see Fig. 5). The three  $^{10}\text{Be}$  exposure age determinations for this ridge sequence are also shown.

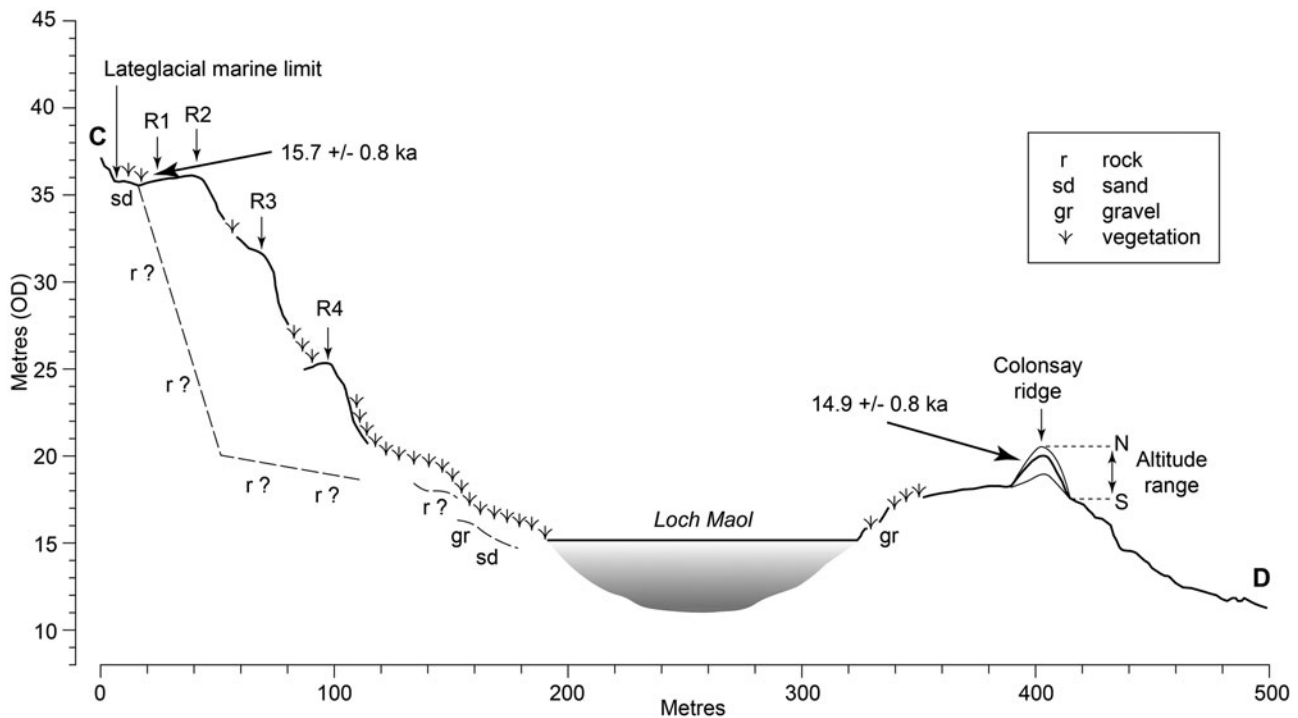


**Figure 8** Cross profile C–D at Shian Bay, seaward from late-glacial marine limit showing the dimensions of the Colonsay Ridge and related <sup>10</sup>Be exposure ages (see also Figs 5, 10; Table 2).

**3.2.3. The Colonsay Ridge.** For most of the W Jura coastline, the lowering of RSL from ~22 m OD to the present coastline cannot be traced below this level as staircases of beach ridges due to the presence of the Main Rock Platform and its backing cliff that post-date the higher ridges. For nearly all areas, this cliff top defines the altitude at which the high beach ridge sequences end. By contrast, the emerged beach ridges that sit on top of this shore platform (itself an emerged feature) are all Holocene in age. One localised area represents an exception to this pattern. At Shian Bay, the cliff top of the Main Rock Platform occurs at ~10 m OD (Fig. 4). Hence, the late-glacial beach ridge staircases in this area represent the only location where the ridges occupy the altitude range between ~22 m and ~10 m OD (Figs 4, 8). In this area, a remarkable linear gravel ridge (the Colonsay Ridge), 480 m in length and aligned N–S, truncates a series of lower ridges almost at right angles and impounds two small lochs ~5 m below the ridge crest (Figs 4, 8). At its northern end, the ridge crest is at 20.3 m OD and thereafter declines in elevation southwards to ~19 m accompanied by a progressive decrease in cobble size. The swale located along the seaward edge of the ridge is at ~18 m and would appear to represent the best approximation to the former position of sea level when the ridge was deposited. Four amalgamated cobbles located at the southern end of this ridge at ~18 m gave a <sup>10</sup>Be exposure age of  $14.9 \pm 0.8$  ka (Fig. 8; Table 2: samples MS01).

**3.2.4. Sgriob na Caillich.** In SW Jura, the Sgriob na Caillich medial moraine descends from Beinn an Oir into Loch na Sgrioba at the seaward margin of which an unvegetated emerged beach truncates the moraine at right angles. A set of four cobbles sampled from the highest beach ridge that truncates the Sgriob na Caillich medial moraine gives an age of  $14.5 \pm 0.8$  ka (Table 2: samples SB1 and SB2). The Sgriob na Caillich moraine itself has a recalculated <sup>10</sup>Be exposure age of  $16.5 \pm 0.8$  ka based on the average of five samples.

**3.2.5. NE Islay.** In NE Islay, two <sup>10</sup>Be exposure ages were determined for glacialfluvial deposits located within the limits of the Coir Odhar moraine (Fig. 9). Here, two outwash samples are located landward and upslope from a clearly defined

late-glacial marine terrace and cliff, the inner edge of which marks the highest level reached by the late-glacial sea in this area (~26.4 m). The two ages for the gravel deposits are  $12.7 \pm 0.6$  ka and  $10.8 \pm 0.4$  ka (Fig. 9; Table 2). In the same area, two dates were obtained from quartzite cobbles on Holocene-emerged beaches at 15 m OD, located below the Main Rock Platform cliff, giving ages of  $4.3 \pm 0.5$  ka and  $3.9 \pm 0.3$  ka (Tables 1, 2).

## 4. Discussion

The <sup>10</sup>Be exposure ages of coastal deposits reported here demonstrate clear interrelationships between the spectacular emerged coastal landforms of W Jura and NE Islay and recent published accounts on the nature of Late Devensian ice sheet deglaciation; they also contribute to our understanding of several aspects of Late Quaternary palaeo-environmental changes in western Scotland. First, the <sup>10</sup>Be exposure ages of the emerged beach ridges and glacialfluvial outwash deposits of W Jura and NE Islay help constrain the nature and timing of Late Devensian ice sheet deglaciation in western Scotland. Second, the shoreline age and altitude data help constrain local and regional patterns of late-glacial RSL change. Third, the age and altitude data of the late-glacial beach ridge sequences provide new information on the timing and rates of glacio-isostatic rebound.

### 4.1. Late Quaternary ice sheet deglaciation

The last (Late Devensian) ice sheet in western Scotland extended as far as the continental shelf (Callard *et al.* 2018), and it is only recently that the nature and timing of regional deglaciation have become clearer. Small *et al.* (2017) presented 17 <sup>10</sup>Be exposure ages of glacially transported boulders and bedrock surfaces that constrain the timing and extent of deglaciation of the marine-based Hebrides ice stream such that by 17–16 ka the ice limit across the Inner Hebrides was likely located close to the present coastline. The ages presented in Small *et al.* (2017) have been recalculated here using the most up-to-date online calculator (v3), producing a mean exposure age of  $16.5 \pm 0.8$  ka for

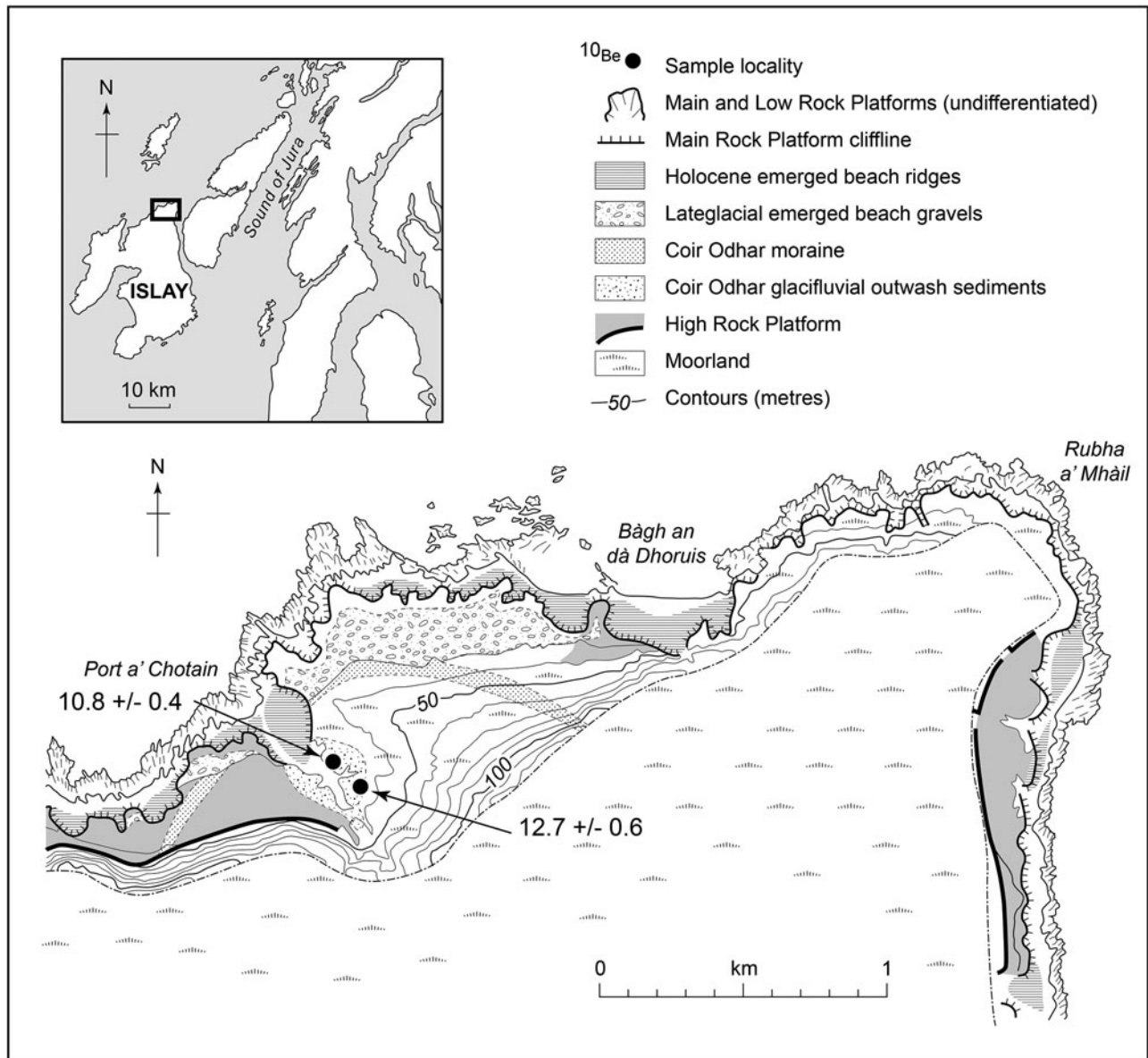


**Figure 9** Geomorphological map of Coir Odhar area, NE Islay, showing partial truncation of outer moraine area by the highest late-glacial emerged marine terrace. The locations of  $^{10}\text{Be}$  exposure samples and ages of alluvial gravels located inside the moraine complex are also shown.

the Sgriob na Caillich medial moraine formation on Jura and a realistic estimate for the local onset of deglaciation. The new data presented here broadly fit with this general picture, despite some acknowledged inheritance issues with large clasts.

On Islay, the  $^{10}\text{Be}$  exposures ages for outwash located inside the Coir Odhar moraine appear to demonstrate deposition during the Loch Lomond Readvance (Younger Dryas). However, the dates provide no conclusive evidence for the age of the moraine ridge itself. Given the size of this moraine together with the absence of any evidence on Jura or Islay of valley glaciation during the Younger Dryas, the most logical explanation is that the moraine likely formed during deglaciation of the last ice sheet and that the outwash inside the moraine was subject to reactivation during the climate deterioration of the Younger Dryas.

Due to an absence of dateable material within the emerged late-glacial marine deposits, Dawson *et al.* (1997) were not able to establish an age for the late-glacial emerged shorelines of W Jura and NE Islay. The  $^{10}\text{Be}$  exposure ages reported here address this issue since ages can be assigned to several emerged beach ridges, the highest of which were deposited immediately following deglaciation (Fig. 10). The ages of  $16.3 \pm 0.9$  ka for the

highest beach ridge at Loch Aoinidh and  $15.7 \pm 0.9$  ka for the highest beach ridge at Shian Bay both point to the deglaciation of W Jura north of Loch Tarbert between  $\sim 15.7$  and  $16.3$  ka, an interpretation in agreement with the  $15.6 \pm 0.9$  ka exposure age from nearby ice-moulded bedrock at the rear of Shian Bay. By contrast, the highest beach ridge in SW Jura at Loch na Sgrioba that truncates the Sgriob na Caillich medial moraine gives an age of  $14.5 \pm 0.8$  ka – approximately 2 ka younger than the reference age of  $16.5 \pm 0.8$  kyr for the moraine itself (Fig. 10). Since the shoreline truncates the moraine, 14.5 ka provides a reasonable constraint for the age of the shoreline.

The dates for the highest beach ridges are in broad agreement with data from an isolation basin farther north at Arisaig, where RSL was located between *ca.* 34 and 36 m OD at  $\sim 16$  cal. kyr BP (Shennan *et al.* 2006, 2018) and with the  $^{14}\text{C}$  age of a basal marine shell from Loch Sunart, NE of Mull, suggesting that this area was also deglaciated prior to  $\sim 16$  cal. kyr BP (Baltzer *et al.* 2010).

#### 4.2. Late-glacial RSL changes

Since the classic research of McCann (1961), the accepted view has been that after the formation of the highest marine terraces



**Figure 10** Aerial panorama, looking SW across the emerged coastal landforms of W Jura, between Shian Bay and Ruantallain (middle distance) (see Fig. 1) with the SW Jura peninsula in the far distance. Superimposed on the photograph are the <sup>10</sup>Be exposure ages (ka) cited in the text. The <sup>10</sup>Be exposure age of the Sgriob na Caillich medial moraine (far distance) is an average value derived from five age determinations. Photograph courtesy of E Smith (photo reference ezc DSC 9774).

across the western isles of Scotland, RSL fell as glacio-isostatic rebound outpaced glacio-eustatic global sea level rise. Here we use the <sup>10</sup>Be age data to constrain the timing and rate of RSL lowering following deglaciation and to better understand the nature of late-glacial glacio-isostatic rebound. Detailed isolation basin research in NW Scotland, together with geophysical modelling, have also addressed this problem (Shennan *et al.* 2006, 2018), and although the field sites described by the latter authors are ~100 km N of western Jura and likely to have experienced slightly different glacio-isostatic rebound histories, the general pattern of late-glacial RSL changes is likely to have been similar for Jura and Islay. This pattern was characterised by a rapid lowering of RSL from the late-glacial marine limit following deglaciation, with the Main Rock Platform having been produced during the Younger Dryas (*ca.* 12.9–11.7 ka).

In W Jura, this late-glacial lowering of RSL was responsible for the sequence of 55 unvegetated beach ridges at Loch Aoinidh that descend from the marine limit at ~35 m to ~25 m OD, terminating at the top of the Main Rock Platform cliff. Three <sup>10</sup>Be ages constrain the nature of this RSL lowering for this area. Following the deposition of the highest ridge at ~36 m OD at 16.3 ± 0.9 ka RSL appears to have fallen with the 25th ridge at ~28 m OD, giving an exposure age of 16.2 ± 0.9 kyr, and ridge 51 at ~21 m OD, giving an exposure age of 15.3 ± 0.8 ka. Broadly interpreted and taking note of the uncertainties associated with these dates, the first *ca.* 15 m of RSL lowering following deglaciation at Loch Aoinidh took place very rapidly over ~1 ka, an interpretation similar to that of Shennan *et al.* (2006, 2018) for the Arisaig area further north.

The late-glacial beach ridge staircase at Shian Bay constitutes the only geomorphological evidence in Scotland demonstrating that significant glacio-isostatic rebound during ice-sheet deglaciation resulted in sustained RSL lowering. Shian Bay is dominated by the Colonsay Ridge that has yielded an exposure age of 14.9 ± 0.8 ka. Notwithstanding that uncertainties in the dating of the ridge prevent a firm correlation, it appears to have broadly coincided with the well-established timing of global meltwater pulse 1A, generally agreed to have taken place sometime between ~14.65 and ~14.8 kyr (Clark *et al.* 2002; Lin

*et al.* 2021). Meltwater Pulse 1A is considered to represent a period of possibly ~500 years when a rapid increase in the rate of glacio-eustatic sea level rise was caused by an acceleration in the rate of melting of northern hemisphere ice sheets. The large size of the Colonsay Ridge compared with adjacent ridges, its high angled truncation of older ridges and its tentative age match with Meltwater Pulse 1A strongly suggest it formed during an interruption (stillstand or reversal) in the progressive lowering of RSL during the late-glacial.

The pattern of RSL change reconstructed from the <sup>10</sup>Be ages of the late-glacial emerged beach ridges in W Jura point to a period of rapid RSL lowering that accompanied ice sheet deglaciation (Fig. 11). Since each date is associated with a relatively large (typically ±900 years) standard error, the emerged shoreline age–altitude plot should be interpreted as an indication of the general trend of RSL following deglaciation. Such caution is further highlighted by the use of swale altitudes in front of each dated beach ridge, since these represent only an approximation of the mean sea level at the time of deposition. In Figure 11, we present the Jura data together with the reconstruction of RSL change for the Arisaig area, NW Scotland (Shennan *et al.* 2006, 2018; Lin *et al.* 2021) (Fig. 11). The plots of late-glacial RSL change are unlikely to be identical across the two areas since they likely experienced slightly different patterns of glacio-isostatic rebound. That said, the similarity in both the overall trend in RSL and the timing of ice-sheet deglaciation for both areas is striking.

## 5. Conclusion

Until recently, our knowledge of the western extent of the Late Devensian ice sheet in Scotland has been mostly based on the results of field mapping and numerical modelling of ice sheet dynamics. Similarly, the nature and timing of ice sheet thinning and retreat have been based on fragmentary geomorphic and stratigraphic evidence (*cf.* Ballantyne & Small 2019). Only with relatively recent <sup>10</sup>Be surface exposure age dating of glacial boulders and bedrock has our understanding of the deglaciation history been transformed. For the Inner Hebrides, it is now

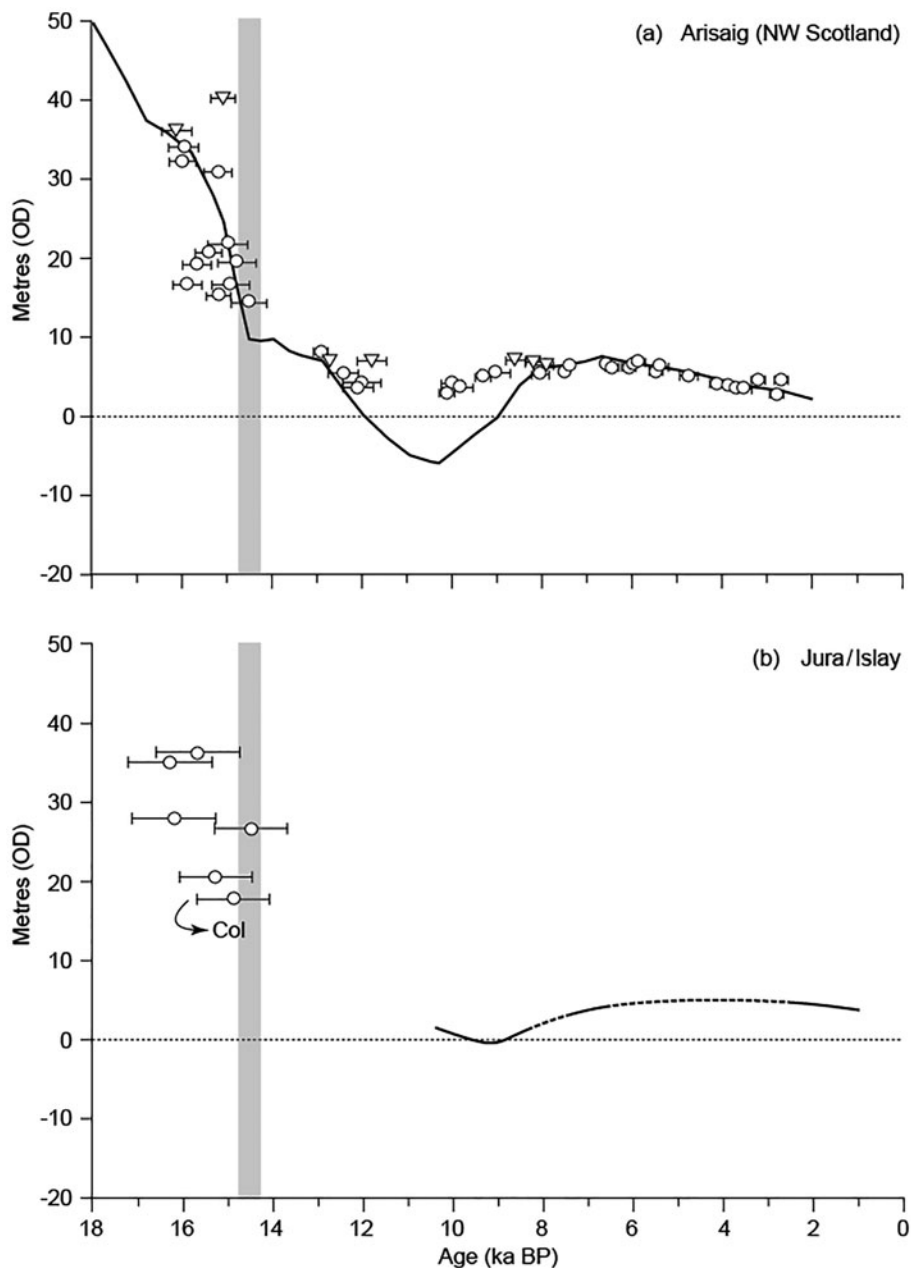


**Figure 11** (a) RSL curve for Arisaig, NW Scotland based on Lin *et al.* (2021) and Shennan *et al.* (2006, 2018). The circled data points and horizontal bars denote the sea level index points and associated standard errors of Shennan *et al.* (2006), while the inverted triangles denote the inferred upper limit of RSL (the late-glacial marine limit). The solid line represents the RSL prediction of Lin *et al.* (2021) using the optimum Earth model, while the shaded vertical bar indicates the approximate age of Meltwater Pulse 1A. (b) Reconstructed trend of RSL for Jura/Islay based on  $^{10}\text{Be}$  age determinations and associated standard error bars presented in this paper, plotted alongside the Holocene RSL curve for Islay (Dawson *et al.* 1998). The possible link between the  $^{10}\text{Be}$  age for the Colonsay Ridge (Col) and Meltwater Pulse 1A is highlighted. Note that the Jura/Islay plot is not an RSL curve *sensu stricto* since the late-glacial altitude values plotted are those from the individual swale depressions in front of the dated gravel ridges. Note that the plots of RSL in the two areas are unlikely to be identical since both are likely to have experienced different patterns of glacio-isostatic rebound.

known that the area was characterised by a major marine-based ice stream (the Hebrides Ice Stream) that drained the last British ice sheet (Small *et al.* 2017). The latter authors demonstrated that by *ca.* 17.5–16.5 ka, the margin of the ice sheet was located across the Inner Hebrides before retreating further. To date, the only empirical evidence of the position of RSL at that time has been from isolation basins at coastal sites in NW Scotland as well as the offshore seismic and stratigraphic research in Loch Sunart (*cf.* Baltzer *et al.* 2010; Shennan *et al.* 2018). Shennan *et al.* (2018) point to the likelihood that the late-glacial marine limit ~100 km N of Jura was in the order of ~35 m OD (almost identical to what it is in W Jura between Ruantallain and Shian Bay) at a time when the ice margin was located nearby. For other areas of the Inner Hebrides, the altitude of the late-glacial

marine limit varies considerably due to differential glacio-isostatic rebound. For example, in Tiree, emerged shore features of the same age as the W Jura features at ~36 m OD, occur between 10 and 11 m OD (Figs 1, 9).

Apart from the isolation basin radiocarbon ages of Shennan *et al.* (2018), the  $^{10}\text{Be}$  exposure ages reported here are the only other known ages from western Scotland that help define the pattern of late-glacial RSL changes that accompanied the retreat and thinning of the Hebridean Ice Stream of the Late Devensian ice sheet. The ages from the highest late-glacial emerged beach ridges (~15.7 to ~16.3 ka) are in general agreement with the dating of the Sgriob na Caillich medial moraine (~16.5 ka) and point to the likelihood that W Jura, between Ruantallain and Shian Bay, was deglaciated around this time. The  $^{10}\text{Be}$  data

reported here indicate that, between ~16.3 ka and the middle of the Younger Dryas (cited here as ~12.1 ka), the area experienced a fall in RSL from *ca.*35 m OD to *ca.*4 m OD equivalent to an *average* rate of RSL lowering of *ca.*7 mmyr<sup>-1</sup>. During this time interval, the uninterrupted fall in RSL is indicated by numerous sets of unvegetated beach ridge staircases. At Shian Bay, however, this relative fall in sea level appears to have been interrupted by the development of the Colonsay Ridge at 14.9 ± 0.8 kyr. It is possible that this ridge was deposited during a brief RSL stillstand of the same general age as global meltwater pulse 1A dated to between ~14.65 and ~14.8 kyr. (Clark *et al.* 2002; Lin *et al.* 2021).

With the exception of the highest beach ridges across W Jura associated with the marine limit, the late-glacial beach ridge staircases are typically represented by low-amplitude ridges separated by shallow swales. For example, the amplitude between individual ridges and adjacent swales in the 55 ridge and swale sequence at Loch Aoinidh is rarely greater than 1 m. By contrast, the staircases of unvegetated Holocene beach ridges and swales are extremely irregular, with amplitude differences greater than 3–4 m not uncommon. This marked contrast supports the view that the evolution of the Holocene gravel ridges was quite different to their late-glacial counterparts, the former having been subject to multiple episodes of gravel recycling, a factor also supported by the wide range in <sup>10</sup>Be exposure ages obtained from individual ridges. By contrast, the late-glacial beach ridge staircases do not exhibit any obvious indication of sustained sediment recycling having taken place. A likely explanation may be that these ridges were deposited during the time interval when the rate of RSL lowering was extremely rapid. This interpretation is well illustrated for the Loch Aoinidh ridge sequence where the formation of 55 ridges within ~1 kyr following deglaciation equates to the production of one ridge per ~20 years.

## 6. Acknowledgements

This research, including <sup>10</sup>Be determinations, was supported by an NERC award (CIAF 9005.04004). We thank Christoph Schnabel for assistance with fieldwork and geochemical processing of samples, and Sandra Mather for cartographic support. Field access and logistic support was kindly provided by Ruantallain and Glenpatrick (Jura) and Islay estates.

## 7. References

- Balco, G. 2013. Alternative calibration data sets. <https://cosmognosis.wordpress.com/2013/10/25/alternative-calibration-data-sets/>.
- Balco, G., Stone, J. O., Lifton, N. A. & Dunai, T. J. 2008. A complete and easily accessible means of calculating surface exposure ages or erosion rates from <sup>10</sup>Be and <sup>26</sup>Al measurements. *Quaternary Geochronology* **3**, 174–95.
- Ballantyne, C. K., Wilson, P., Gheorgiu, D. & Rodes, A. 2014. Enhanced rock-slope failure following ice-sheet deglaciation: timing and causes. *Earth Surface Processes and Landforms* **39**, 900–13.
- Ballantyne, C. K. & Dawson, A. G. 2019. Scottish Landform examples 45: Sgriob na Caillich: a landslide-sourced medial moraine on the isle of Jura. *Scottish Journal of Geography* **135**, 139–49.
- Ballantyne, C. K. & Small, D. 2019. The last Scottish ice sheet. *Earth and Environmental Science Transactions of the Royal Society of Edinburgh* **110**, 93–131.
- Baltzer, A., Bates, R., Mokeddem, Z., Clet-Pellerin, M., Walter-Simonnet, A. V., Bonnot-Courtois, C. & Austin, W. E. 2010. Using seismic facies and pollen analyses to evaluate climatically-driven change in a Scottish sea loch (fjord) over the last 20 Ka. *Geological Society of London Special Publication* **334**, 355–69.
- Borchers, B., Marrero, S., Balco, G., Caffee, M., Goehring, B., Lifton, N., Nishiizumi, K., Phillips, F., Schaefer, J. and Stone, J. 2016. Geological calibration of spallation production rates in the CRONUS-earth project. *Quaternary Geochronology* **31**, 188–98.
- Callard, S. L., Cofaigh, C. O., Benetti, S., Chiverrell, R. C., Van Landeghem, K. J., Saher, M. H., Gales, J. A., Small, D., Clark, C. D., Stephen, J. L. & Fabel, D. 2018. Extent and retreat history of the Barra Fan Ice stream offshore western Scotland and northern Ireland during the last glaciation. *Quaternary Science Reviews* **201**, 280–302.
- Clark, P. U., Mitrovica, J. X., Milne, G. & Tamisiea, M. 2002. Sea-level fingerprinting as a direct test for the source of global meltwater pulse 1A. *Science* **5564**, 2438–41.
- Dawson, A. G. 1979. *Raised shorelines of Jura, Scarba and NE Islay*. Unpublished PhD Thesis, University of Edinburgh.
- Dawson, A. G. 1980. Shore erosion by frost: an example from the Scottish Lateglacial. In Lowe, J. J., Gray, J. M. & Robinson, J. E. (eds) *Studies in the Lateglacial of NW Europe*, 45–53. Oxford: Pergamon Press.
- Dawson, A. G. 1982. Lateglacial sea-level changes and ice-limits in Islay, Jura and Scarba, Scottish Inner Hebrides. *Scottish Journal of Geology* **18**, 253–65.
- Dawson, A. G., Dawson, S., Foster, I. D. L., Tooley, M. J., Brookes, C. & Smith, D. E. 1997. Lateglacial relative sea level changes, Ruantallain-Shian Bay, western Jura. In Dawson, A. G. & Dawson, S. (eds) *The Quaternary of Islay and Jura, Quaternary Research Association field guide*, 17–41. Melton Mowbray: Marble Press.
- Dawson, S., Dawson, A. G. & Edwards, K. J. 1998. Rapid Holocene relative sea-level changes in Gruinart, Isle of Islay, Scottish Inner Hebrides. *The Holocene* **8**, 183–95.
- Dunne, J., Elmore, D. & Muzikar, P. 1999. Scaling factors for the rates of production of cosmogenic nuclides for geometric shielding and attenuation at depth on sloped surfaces. *Geomorphology* **27**, 3–11.
- Fabel, D., Ballantyne, C. K. & Xu, S. 2012. Trimlines, blockfields, mountain-top erratics and the vertical dimensions of the last British-Irish Ice sheet in NW Scotland. *Quaternary Science Reviews* **55**, 91–102.
- Freeman, S., Bishop, P., Bryant, C., Cook, G., Dougans, D., Ertunc, T., Fallick, A., Ganeshram, R., Maten, C., Naysmith, P., Schnabel, C., Scott, M., Summerfield, M. & Xu, S. 2007. The SUERC AMS laboratory after 3 years. *Nuclear Instruments and Methods in Physics Research B* **259**, 66–70.
- Fulop, R. H., Bishop, P., Fabel, D., Cook, G., Everest, J., Schnabel, C., Codilean, A. T. & Xu, S. 2015. Quantifying soil loss with in-situ cosmogenic <sup>10</sup>Be and <sup>14</sup>C depth-profiles. *Quaternary Geochronology* **27**, 78–93.
- Holmes, A. 1965. *Principles of physical geology*. 3rd edn, London: Thomas Nelson and Sons.
- Johnson, D. W. 1922. *Shore processes and shoreline development*. New York: Wiley.
- Kohl, C. P. & Nishiizumi, K. 1992. Chemical isolation of quartz for measurement of *in situ*-produced cosmogenic nuclides. *Geochimica Acta* **56**, 3583–87.
- Lambeck, K., Rouby, H., Purcell, A., Sun, Y. & Sambridge, M. 2014. Sea level and global ice volumes from the Last Glacial Maximum to the Holocene. *Proceedings of the National Academy of Sciences* **111**, 15296–303.
- Lifton, N., Sato, T., and Dunai, T. J. 2014. Scaling in situ cosmogenic nuclide production rates using analytical approximations to atmospheric cosmic-ray fluxes. *Earth and Planetary Science Letters* **386**, 149–160.
- Lin, Y., Hibbert, F. D., Whitehouse, P. L., Woodroffe, S. A., Purcell, A., Shennan, I. & Bradley, S. L. 2021. A reconciled solution of Meltwater Pulse 1A sources using sea-level fingerprinting. *Nature Communications*, **12**, 2015.
- Lowe, J. J., Matthews, I., Mayfield, R., Lincoln, P., Palmer, A., Staff, R. & Timms, R. 2019. On the timing of retreat of the Loch Lomond ('Younger Dryas') Readvance icefield in the SW Scottish Highlands and its wider significance. *Quaternary Science Reviews* **219**, 171–86.
- MacLeod, A., Palmer, A., Lowe, J. J., Rose, J., Bryant, C. and Merritt, J. 2011. Timing of glacier response to Younger Dryas climatic cooling in Scotland. *Global and Planetary Change* **79**, 264–74.
- McCann, S. B. 1961. *The raised beaches of western Scotland*. Unpublished PhD Thesis, University of Cambridge.
- McCann, S. B. 1964. The raised beaches of north-east Islay and western Jura, Argyll. *Transactions of the Institute of British Geographers* **35**, 1–16.
- Nishiizumi, K., Imamura, M., Caffee, M. W., Southon, J. R., Finkel, R. C. & Mccann, J. 2007. Absolute calibration of Be-10 AMS standards. *Nuclear Instruments and Methods in Physics Research B* **258**, 403–13.
- Peach, B. N., Wilson, J. S. G., Hill, J. B., Bailey, E. B. & Graham, G. W. 1911. The geology of Knapdale, Jura, and North Kintyre. Memoir of the Geological Survey of Great Britain.

- Shennan, I., Hamilton, S., Hillier, C., Hunter, A., Woodall, R., Bradley, S., Milne, G., Brooks, A. & Bassett, S. 2006. Relative sea-level observations in western Scotland since the last glacial maximum for testing models of glacial isostatic land movements and ice-sheet reconstructions. *Journal of Quaternary Science* **21**, 601–13.
- Shennan, I., Bradley, S. L. & Edwards, R. 2018. Relative sea level changes and crustal movements in Britain and Ireland since the last glacial maximum. *Quaternary Science Reviews* **188**, 143–59.
- Small, D., Benetti, S., Dove, D., Ballantyne, C. K., Fabel, D., Clark, C. D., Gheorghiu, D. M., Newall, J. & Sheng, X. 2017. Cosmogenic exposure age constraints on deglaciation and flow behaviour of a marine-based ice stream in western Scotland, 21–16 ka. *Quaternary Science Reviews* **167**, 30–46.
- Syngé, F. M. & Stephens, N. 1966. Late- and Post-glacial shorelines and ice limits in Argyll and Northeast Ulster. *Transactions of the Institute of British Geographers* **39**, 101–25.
- Stone, J., Lambeck, K., Fifield, L. K., Evans, J. T. & Cresswell, R. G. 1996. A lateglacial age for the Main Rock Platform, western Scotland. *Geology* **24**, 707–10.
- Wright, W. B. 1928. The raised beaches of the British Isles. *First report of the Commission on Pliocene and Pleistocene Terraces, International Geographical Union*, 99–106.
- Xu, S., Dougans, A. B. & Freeman, S. 2010. Improved  $^{10}\text{Be}$  and  $^{26}\text{Al}$  AMS with a 5 MV spectrometer. *Nuclear Instruments & Methods in Physics Research, B: Beam Interactions with Materials and Atoms* **268**, 737–38.

---

MS received 12 November 2021. Accepted for publication 9 June 2022. First published online 8 September 2022